



# OPEN Synbiotics as a novel therapeutic approach for hyperphosphatemia and hyperparathyroidism in chronic kidney disease rats

Weerapat Anegkamol<sup>1</sup>, Wirin Bowonsomsarit<sup>1</sup>, Mana Taweewisit<sup>2</sup>, Somying Tumwasorn<sup>3</sup>, Thana Thongsricome<sup>4</sup>, Maroot Kaewwongse<sup>5</sup>, Rath Pitchyangkura<sup>6</sup>, Piyaratana Tosukhowong<sup>1</sup>, Natthaya Chuaypen<sup>1</sup> & Thasinas Dissayabutra<sup>1✉</sup>

Hyperphosphatemia and secondary hyperparathyroidism (SHPT) are the common complications found in CKD that lead to severe complications including mineral bone disease (MBD), vascular calcification (VC), and cardiovascular mortality. To mitigate hyperphosphatemia, SHPT and uremic toxemia, we supplemented cisplatin-induced CKD rats with a synbiotic composed of *Lactobacillus salivarius* LBR228, *Bifidobacterium longum* BFS309, fructo-oligosaccharide and chitosan oligosaccharide, with *Lactobacillus casei* as a standard probiotic control. After the 12 weeks experiment, rats supplemented with the synbiotic had lower serum phosphate, calcium-phosphorus product, serum parathyroid hormone, and indoxyl sulfate levels than untreated rats. The expression of type 1 RNA and protein expression were increased in rats treated with the synbiotics. Our result showed that synbiotic treatment alleviates hyperphosphatemia and SHPT, which are the main risks of MBD and VC. The mode of the synbiotic action is hypothesized to associate with the improvement of the tight junction and gut barrier, leading to the suppression of intestinal paracellular phosphate transport. This study demonstrated the beneficial effects of synbiotic treatment in the control of serum phosphate and parathyroid hormone in an animal model with CKD.

**Keywords** Synbiotics, Phosphate, Chronic kidney disease, Hyperparathyroidism, Tight junction, Paracellular transport

## Background & summary

Chronic kidney disease (CKD) affects more than 10% of the population worldwide, with increasing prevalence of disease, and the global health burden. CKD is accompanied by several morbid complications, one of which is secondary hyperparathyroidism (SHPT). SHPT in CKD caused by vitamin D deficiency and hyperphosphatemia and is responsible for metabolic bone disease (CKD-MBD) and vascular calcification (VC), leading to cardiovascular death. The International Kidney Disease: Improving Global Outcomes (KDIGO) work group convened this issue and established the guideline in 2017 to control SHPT taking into account the development of VC, suggesting to restrict hyperparathyroidism treatment using calcium-based or active vitamin D to regulate normal serum calcium and lower the progression of VC<sup>1</sup>. Thus, non-calcium phosphate binders, calcimimetics, and new agents such as ferric citrate and tenapanor were introduced<sup>2–4</sup>.

The etiology of hyperphosphatemia in CKD is multifactorial: increased intestinal phosphate absorption, bone turnover, and renal phosphate absorption<sup>5</sup>. Most traditional interventions aim to reduce intestinal phosphate absorption, such as dietary phosphate restriction and phosphate binders. While calcimimetic, vitamin D, and

<sup>1</sup>Metabolic Disease in Gastrointestinal and Urinary System Research Unit, Department of Biochemistry, Faculty of Medicine, Chulalongkorn University, Bangkok 10330, Thailand. <sup>2</sup>Department of Pathology, Faculty of Medicine, Chulalongkorn University, Bangkok 10330, Thailand. <sup>3</sup>Department of Microbiology, Faculty of Medicine, Chulalongkorn University, Bangkok 10330, Thailand. <sup>4</sup>Department of Physiology, Faculty of Medicine, Chulalongkorn University, Bangkok 10330, Thailand. <sup>5</sup>Division of Physiology, School of Medical Sciences, University of Phayao, Phayao 56000, Thailand. <sup>6</sup>Department of Biochemistry, Faculty of Science, Chulalongkorn University, Bangkok 10330, Thailand. ✉email: thasinas@chula.md

parathyroidectomy aim to suppress the serum parathyroid level. Focusing on intestinal absorption, recent evidence indicated that paracellular transport is the main route of phosphate entry under conditions of normal to high phosphate availability<sup>6,7</sup>. Regulation of paracellular transport using a sodium/hydrogen exchanger inhibitor was shown to efficiently reduce serum phosphate in human<sup>8</sup>.

Yang et al reported that most CKD patients had intestinal microbial disturbance, called gut dysbiosis, due to multifactorial factors such as intestinal edema, increased intestinal lumen pH due to ammonium secretion, diet and drugs<sup>9</sup>. Gut dysbiosis causes gut barrier leakage by down-regulation of epithelial tight junction proteins, leading increased paracellular transport, hyperphosphatemia<sup>10</sup>. Alteration of gut microbiome also promotes uremic toxins, endotoxins, inflammation, and bacterial translocation, contributing to the progression of kidney disease<sup>11</sup>.

Improvement of gut dysbiosis by food or biotic intervention was able to slow the progression of CKD<sup>12</sup>. Our previous study using prebiotics treatment in rats with CKD improved the the gut microbiota population and intestinal barrier protein, as well as decreased serum uremic toxin<sup>13,14</sup>. In order to this, we aimed to use a synbiotic composed of *Lactobacillus salivarius*, *Bifidobacterium longum*, chitosan oligosaccharide (COS) and inulin to suppress intestinal phosphate absorption, by modulating the gut microbiota and gut barrier promotion. We anticipate that this novel synbiotic could be used as an adjuvant therapy in the treatment of hyperphosphatemia and SHPT.

## Materials and methods

### Animal study

Male Wistar rats were purchased from Nomura Siam Co. Ltd. and is housed at the Animal Laboratory Center, Faculty of Medicine, Chulalongkorn University. The rats were kept under controlled conditions, 25 °C temperature with a 12/12-hour light/dark cycle and had free access to food and water. They were acclimatized for 14 days before starting the experiments. Chronic kidney disease (CKD) was induced in all CKD groups through a peritoneal injection of cisplatin at a dose of 8 mg / kg body weight, while control was injected with normal saline. For chronic kidney injury induction, 1% w/v phosphoric acid was added to the drinking water, which was adjusted to a pH of 6.5 to 7.0. After induction, the animals were randomly divided into four groups ( $n=8$  per group): (1) Naive control (Control), (2) CKD control (CKD), (3) CKD treated with *Lactobacillus casei* as standard probiotic (STDPro) and (4) CKD treated with a synbiotic formulation of COS, inulin, *Bifidobacterium longum* strain BFS309, and *Lactobacillus salivarius* strain LBR228 (Synbiotics). Body weight and drinking volume were measured every two weeks. Blood was drawn at week 0 (2 weeks after cisplatin induction of kidney injury), 4, 8 and 12, using isoflurane as an anesthetic drug.

In the present study, Control and CKD rats were gavaged with PBS, while Synbiotic rats were fed with  $10^9$  colony forming units (CFU) of *Bifidobacterium longum* BFS309 and *Lactobacillus salivarius* LBR228, and STDPro rats with  $10^9$  CFU of *L. casei*. In addition, 150 mg of inulin (Banpong Novitat, Thailand), and 25 mg of COS (kindly contributed by Asst. Prof.Dr.Rath Pitchyangura), were mixed and gavaged with probiotics in both the Synbiotic and STDPro groups. The total volume of mixed probiotics and prebiotics was approximately 0.5 mL dail, and the duration of the experiment was 12 weeks.

Body weight, water and food intake was recorded at week 0, 4, 8, and 12. At the end of the experimental period, all rats were sacrificed by overdosing with isoflurane inhalation, and their blood, kidney, intestine, and intestinal feces were collected.

### Serum biochemistry

Serum creatinine, calcium, and phosphate levels were measured using the Alinity ci system (Abbott Laboratories, IL, USA). Serum total parathyroid hormone (PTH) levels were quantified using an ELISA kit (Wuhan Fine Biotech Co., Ltd.) using absorbance readings at 450 nm according to the manufacturer's guideline. The indoxyl sulfate levels were analyzed at the Center for Medical Diagnostic Laboratories, Faculty of Medicine, Chulalongkorn University, King Chulalongkorn Memorial Hospital using the HPLC technique<sup>15</sup>.

### Histopathological evaluation

Tissue processing was conducted at the Department of Pathology, Faculty of Medicine, Chulalongkorn University. Kidney and jejunum sections were stained with hematoxylin and eosin (H&E) for histopathological evaluation. Kidney injury and fibrosis were assessed using established scoring systems. For renal tissue assessment, five stained sections from each rat were evaluated based on the following criteria: vacuolization of proximal tubular cells, red blood cell congestion, leukocyte infiltration, eosinophilic casts, necrosis of proximal tubular cells, and bleeding. The extent of acute renal tubular necrosis was then determined using a semiquantitative scoring method as follows: normal (0 points), < 10% damage (1 point), 10–25% damage (2 points), 26–75% damage (3 points), and > 75% damage (4 points)<sup>16</sup>.

Histopathological changes in the jejunal epithelial were evaluated according to the Marsh classification<sup>17</sup>. The immunohistochemistry of the jejunal tight junction protein was evaluated using anti-ZO1 antibody (Thermo Fisher, Massachusetts, USA, Catalog # 61–7300).

### Expression of tight junction expression

To assess integrity of the intestinal epithelial barrier, total RNA was extracted from jejunum tissue using TRIzol™ reagent (Thermo Fisher, Massachusetts, United States). Briefly, the tissue was homogenized in TRIzol™ reagent to lyse the cells and release RNA. Chloroform was then added to separate the mixture into aqueous and organic phases. Total RNA was isolated from the aqueous phase, precipitated with isopropanol, and the resulting pellet was washed with 75% ethanol. After briefly air-drying, the total RNA was dissolved in RNase-free water and quantified for further analysis. The extracted RNA from the samples was then subjected to q-RT-PCR analysis

for the expression of Occludin and Zonula Occludens-1 (ZO-1). The expression of each tight junction protein was calculated relative to the GAPDH, the housekeeper. The relative expression was calculated by fold changes from the control. The primers for PCR are shown in Table 1.

Fecal microbiome analysis

Microbial DNA was extracted from fecal samples using the ZymoBIOMICS DNA Miniprep Kit and assessed for purity and concentration were assessed with a DeNovix UV-vis spectrophotometer. The DNA samples were prepared for target sequencing in the V3-V4 hypervariable region of the 16 S rRNA gene. Target sequences were amplified, and the DNA library was quantified. Positive controls for library preparation and negative controls were included to assess the level of bioburden introduced during the process. Microbiome profiling utilized the 16 S / ITS microbiome profiling service (Illumina® MiSeq™ system). The analysis included demultiplexing, DADA2 processing for the generation of ASV tables, and taxonomy assignment with QIIME v.1.9.1. Microbial diversity was analysed using ecological indices and PCoA plots, with relative abundances correlated with physiological data.

Statistical analysis

Data analysis was performed using SPSS version 22.0. (IBM statistics, USA) Data were presented as mean ± standard deviation unless otherwise indicated. Continuous data were analyzed using Student’s t-test, ANOVA with Bonferroni post hoc test, and Mann-Whitney U test for nonparametric data. The Kruskal-Wallis test and chi-square test were employed for nonparametric group comparisons and histological analyses, respectively. Pearson’s correlation was used to examine relationships between variables. Statistical significance was established at *p* < 0.05. The figures demonstrated in the present study were generated by GraphPad Prism ver 10.0 (Boston, MA).

Ethical consideration

The study was carried out according to the Helsinki Declaration and Good Clinical Practice guidelines for participants who provided fecal samples. For the experimental animals, all procedures adhered to the guidelines of the Institutional Animal Care and Use Committee (IACUC) and ARRIVE. The study procedures were approved by the Institutional Review Board of the Faculty of Medicine, Chulalongkorn University, approval number 914/64. The protocols for the animal experiments were approved by the Chulalongkorn University Animal Care and Use Committee, protocol number 004/2563.

Results

Rats’ wellbeing

The general health status of the animals was monitored throughout the study. The body weight of the rats in each group was recorded every 4 weeks. The body weight of Control group was slightly higher than that of all CKD groups after the CKD-induction phase, however, the difference was not statistically significant during the experiment (Figure S1). Food and water intake remained comparable across all groups, with no significant differences observed as shown in the supplementary Figure S1b and Figure S1c.

Serum biochemistry and uremic toxin levels

Two weeks after induction of kidney injury with cisplatin, serum creatinine levels in all groups of CKD were significantly elevated compared to the Control and gradually increased until the end of the experiment (Fig. 1a). There was no difference in serum creatinine levels between each CKD group.

Serum phosphate was markedly elevated in CKD groups compared to the Control group throughout the experiment (Fig. 1b). Initially, serum phosphate levels in the STDPro and Synbiotic groups were normal, but gradually increased at weeks 8 and 12. At the end of the experiment, Synbiotics treated rats had significantly lower serum creatinine compared to CKD rats, (approximately 29.04% reduction) and comparable with Control rats. Serum calcium levels did not differ among groups at week 12 (Fig. 1c).

At the end of the study, the calcium-phosphorus product (Ca × P) in the Synbiotic group was significantly lower compared to the CKD group (Fig. 1d). Similarly, serum PTH levels were markedly increased in CKD and STDPro rats, while Synbiotic treated rats had significantly lower PTH levels than CKD rats, with levels comparable to Control rats (Fig. 1e). Furthermore, Synbiotic treated rats had lower serum indoxyl sulfate levels than CKD rats, with levels comparable to Control rats at week 12 (Fig. 1f).

Target	Primer	Sequence	Product size (bp)
GAPDH <sup>18</sup>	Forward	GTGAAGGTCGGAGTCAACGG	104
	Reverse	TCGATGAAGGGTCATTGATGG	
Occludin <sup>19</sup>	Forward	CCAATGTCGAGGAGTGGG	237
	Reverse	CGCTGCTGTAACGAGGCT	
Zonula occludens <sup>20</sup>	Forward	CCAATGTCGAGGAGTGGG	183
	Reverse	CGCTGCTGTAACGAGGCT	

Table 1. Sequence of PCR primers for RT-qPCR and product sizes.

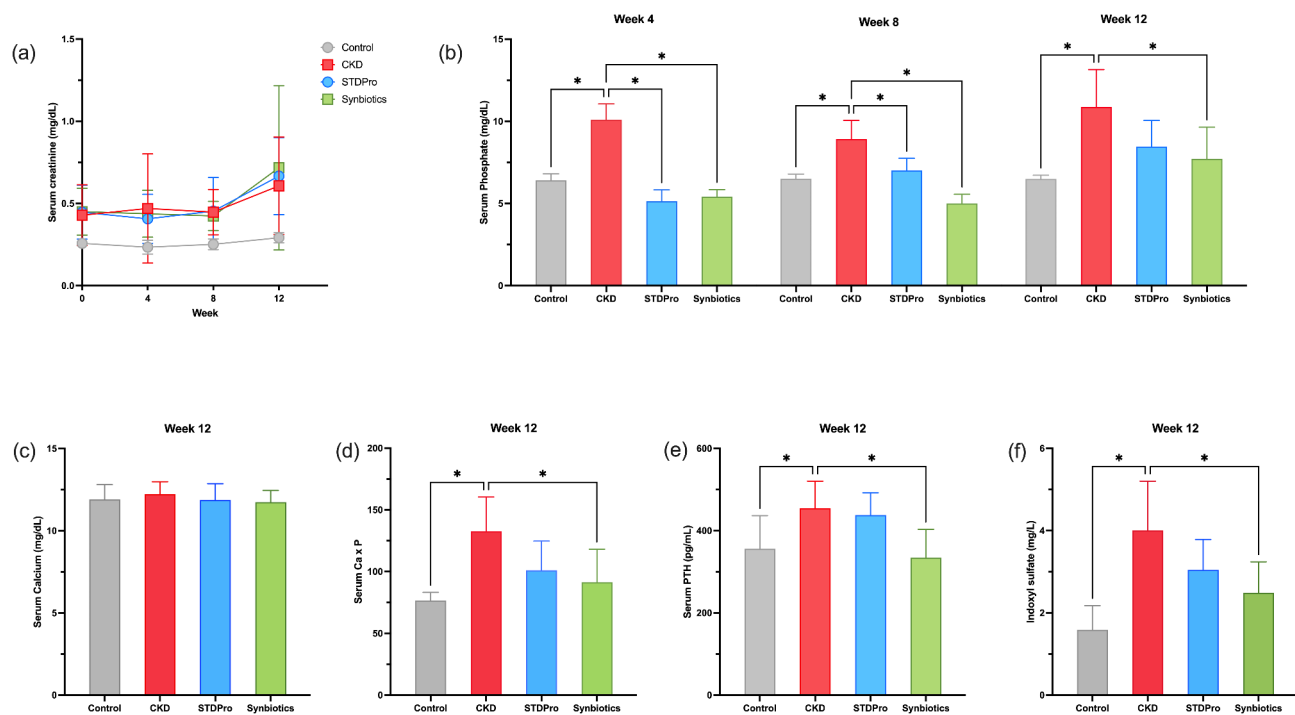


**Fig. 1.** Serum biochemistry levels. (a) Serum creatinine levels during week 0 to week 12. (b) Serum phosphate levels during week 4 to week 12. (c) Serum calcium levels at week 12. (d) Serum calcium-phosphorus products at week 12. (e) Serum levels of parathyroid hormone (PTH) at week 12 and (f) Serum indoxyl sulfate levels at week 12. Data are presented as mean  $\pm$  SD. \* $P < 0.05$ .

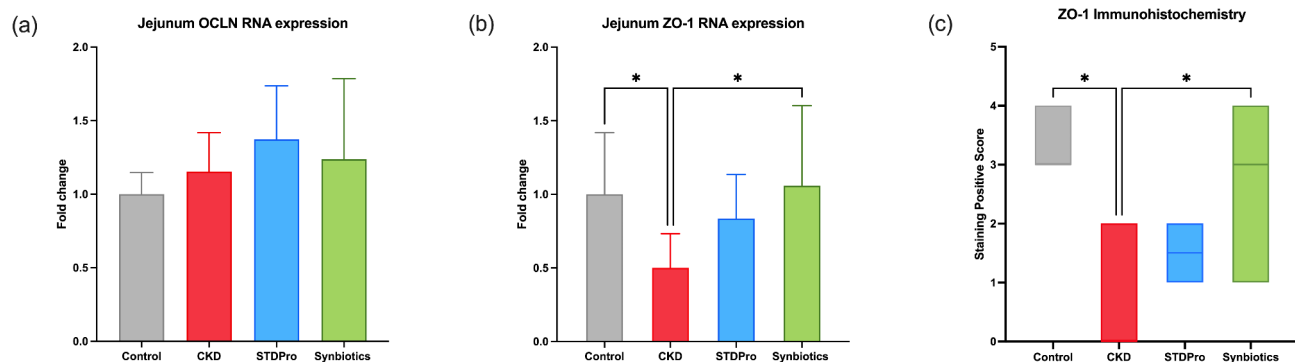


**Fig. 2.** Expression of tight junction markers in the epithelial tissue of the jejunum of rats. (a) RNA expression of the occludin gene (OCLN), as determined by qRT-PCR. Relative expression levels are normalized to a housekeeping gene and presented as mean  $\pm$  SD., (b) RNA expression of the zonula occludens-1 (ZO-1) gene, determined by qRT-PCR. The relative expression levels are normalized to a housekeeping gene and are presented as mean  $\pm$  SD., and (c) Immunohistochemical staining of the ZO-1 protein in jejunal epithelial tissue was evaluated using a histological scoring system. The scoring was based on the percentage of the positive staining area of the anti-ZO-1 antibody at the epithelial tight junctions. A score of 0 was assigned when the positive staining area was  $< 10\%$ , score 1 for 10–25%, score 2 for 26–50%, score 3 for 51–75%, and score 4 for  $> 75\%$  positive staining. Data are presented in a box plot showing the Min-Max score with the median. Statistical significance is indicated where applicable. \* $p < 0.05$ .

### Histopathological examination

Notable histopathological changes were present in the kidneys of all cisplatin-induced CKD groups, including tubular necrosis, glomerular necrosis, and multiple tubular dilations, as illustrated in the Supplementary Figure S2. The glomerular lesion scores did not show significant differences between the CKD, STDPro and Synbiotics groups.

The expression levels of occludin (OCLN) were not statistically different between each group (Fig. 2a). However, the expression of ZO-1 was significantly decreased in the CKD group compared to the Control group.

Synbiotic treatment restored ZO-1 expression to levels comparable to those observed in the Control group (Fig. 2b).

Immunohistochemical analysis of the jejunum, shown as positive staining with anti-ZO-1 in Fig. 3c, and tissue staining was demonstrated in Supplementary Figure S3, confirmed significantly higher ZO-1 expression in the synbiotics group compared to the CKD group. Quantitative analysis of ZO-1 expression, represented as histological scoring, is shown in Fig. 2c. No significant differences in ZO-1 RNA or protein expression were observed between the CKD and STDPro groups.

### Gut microbiota analyses

The gut microbiota analysis was conducted at the end of the experiment to assess the diversity within the microbial communities of the experimental groups. Alpha diversity indices, including Shannon's, Faith's phylogenetic diversity and Pielou's evenness indices, were not significantly different between each group, indicating similar microbial diversity and evenness between samples (Fig. 3a and b, and Fig. 3c, respectively). The relative abundances of the fecal microbiota were analyzed between experimental groups. Stacked bar graphs depict the proportions of bacterial phyla and genera (Fig. 3d and e).

Principal Coordinate Analysis (PCoA) based on Bray-Curtis dissimilarity was performed to evaluate differences in gut microbiota composition among the experimental groups. As shown in Fig. 4, significant clustering of gut microbiota profiles was observed between the CKD group and other experimental groups (PERMANOVA,  $p < 0.05$ ). Each point in the PCoA plot represents an individual sample, with distinct colors indicating group membership. The analysis revealed significant differences in gut microbiota composition between the CKD group and the control group ( $p < 0.05$ ), as well as between the CKD group and the Synbiotics group ( $p < 0.05$ ).

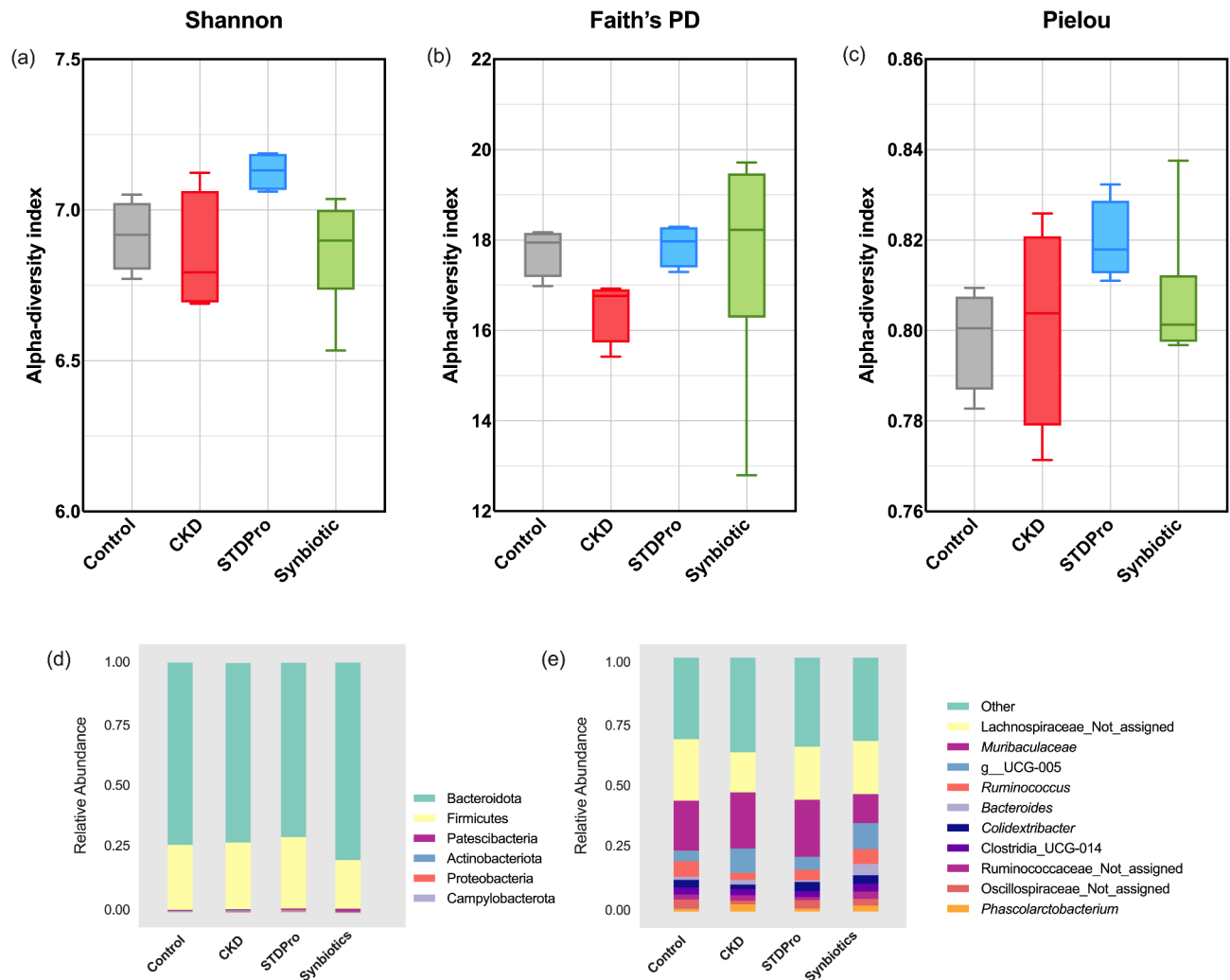
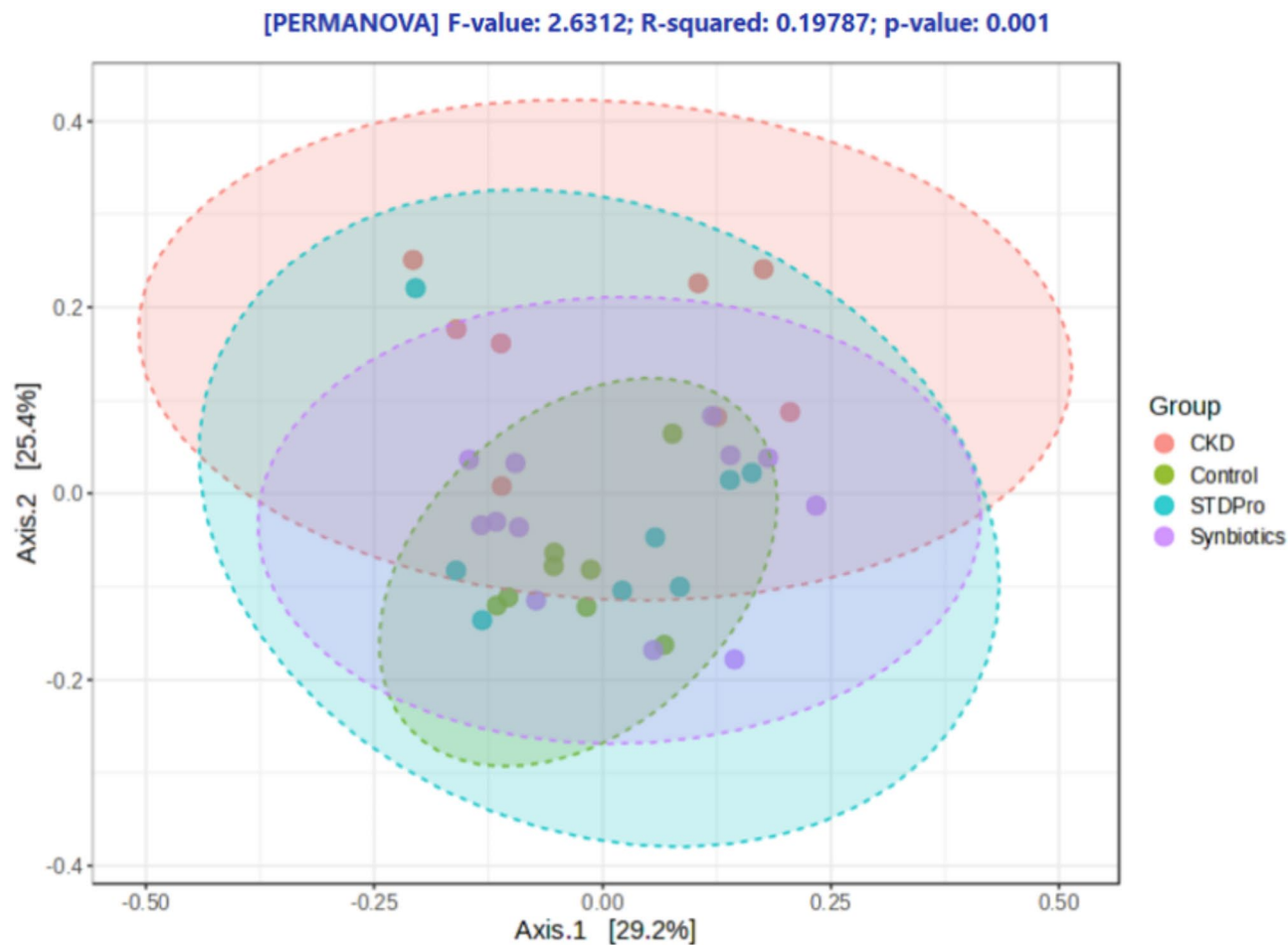


**Fig. 3.** Analysis of the gut microbiota illustrating diversity and composition between experimental groups. (a) Shannon diversity index, (b) Faith's phylogenetic diversity (PD), (c) Pielou's evenness, (d) relative abundance at the phylum level and (e) relative abundance at the genus level. Box-and-whisker plots are presented as median  $\pm$  IQR, with whiskers representing the minimum and maximum values.



Compare	F-value	R-squared	P-value	FDR
CKD vs Control	5.2546	0.2729	0.002	0.012
CKD vs STDPro	2.54	0.15357	0.053	0.0795
CKD vs Synbiotics	3.3991	0.15884	0.006	0.018

**Fig. 4.** Principal Coordinate Analysis (PCoA) of the composition of the gut microbiota comparing the CKD group with other experimental groups. The analysis is based on Bray-Curtis dissimilarity, and significant clustering was observed between groups (PERMANOVA,  $p < 0.05$ ). Each point represents an individual sample, with colors indicating group membership.

Table 2 demonstrated the comparison between the change in the gut microbiota (week 12 vs. week 0) between CKD and Synbiotic rats. Our study found that synbiotic treatment could suppress the relative abundance of 11 bacterial genera, such as the Prevotellaceae\_NK3B31 and UCG001 groups, *Lachnospiraceae\_NK4A136*, *Roseburia*, etc. Furthermore, 18 genera were relatively increased by synbiotic therapy including *Bacteroides*, *[Eubacterium]\_fissicatena*, *Oscillospira*, *Butyricimonas*, *Phascolarctobacterium*, *Allobaculum* and *Lactobacillus*.

Discussion

The tight junction protein complex is an important structure for controlling paracellular transport. It is well recognized that gut dysbiosis leads to suppression of tight junction protein expression<sup>21,22</sup>. In patients with CKD, gut dysbiosis also causes the production of uremic toxins, such as indole, p-cresol and trimethylamine (TMA), endotoxins, and inflammatory cytokines. With leaky gut barriers, the absorption of these toxins, as well as phosphate, is enhanced, further damage kidney and various tissues. Mineral bone disease (MBD) and VC are the serious complications of hyperphosphatemia and SHPT<sup>23</sup>. According to the KDIGO guideline 2017, the use of any phosphate-lowering drugs that cause hypercalcemia should be sanitized or avoided due to the risk of VC development<sup>24</sup>.



	Median $\pm$ IQR	p-value
Depleted Genera		
Prevotellaceae_NK3B31_group	-5.736 $\pm$ 3.494	0.028
Prevotellaceae_UCG-001	-5.051 $\pm$ 2.978	0.028
Lachnospiraceae_NK4A136_group	-3.155 $\pm$ 3.537	0.028
<i>Roseburia</i>	-1.820 $\pm$ 1.484	0.046
<i>Akkermansia</i>	-1.580 $\pm$ 1.339	0.028
<i>Lachnoclostridium</i>	-0.400 $\pm$ 0.371	0.028
UCG-009	-0.318 $\pm$ 0.291	0.028
<i>Clostridium sensu stricto</i> _1	-0.292 $\pm$ 0.401	0.028
GCA-900,066,575	-0.078 $\pm$ 0.108	0.046
Lachnospiraceae_FCS020_group	-0.032 $\pm$ 0.052	0.043
Lachnospiraceae_UCG-006	-0.019 $\pm$ 0.207	0.027
Enriched Genera		
<i>Anaerovorax</i>	0.035 $\pm$ 0.063	0.042
<i>Muribaculum</i>	0.035 $\pm$ 0.039	0.026
[ <i>Eubacterium</i> ] <i>_fissicatena_group</i>	0.104 $\pm$ 0.279	0.028
<i>Negativibacillus</i>	0.108 $\pm$ 0.225	0.046
<i>Oscillospira</i>	0.112 $\pm$ 0.346	0.046
<i>Butyrivimonas</i>	0.164 $\pm$ 0.186	0.028
<i>Sellimonas</i>	0.238 $\pm$ 0.136	0.042
<i>Allobaculum</i>	0.320 $\pm$ 0.331	0.028
<i>Elusimicrobium</i>	0.350 $\pm$ 0.548	0.028
Christensenellaceae_R-7_group	0.421 $\pm$ 0.495	0.046
<i>Alloprevotella</i>	0.450 $\pm$ 0.551	0.028
<i>Candidatus saccharimonas</i>	0.521 $\pm$ 1.152	0.028
<i>Monoglobus</i>	1.126 $\pm$ 1.486	0.046
[ <i>Eubacterium</i> ] <i>_coprostanoligenes_group</i>	1.517 $\pm$ 0.906	0.028
<i>Acetitomaculum</i>	1.580 $\pm$ 2.107	0.028
<i>Phascolarctobacterium</i>	1.666 $\pm$ 1.981	0.028
<i>Bacteroides</i>	2.671 $\pm$ 4.000	0.028
UCG-005	7.560 $\pm$ 5.924	0.028

**Table 2.** Change in the gut microbiota in CKD rats treated to synbiotics compared with CKD rats. Data were present in the median  $\pm$  interquartile range and only bacterial taxa with significant change were present.

Our team believed that probiotic/synbiotic is a key to alleviating the severity of these complications in CKD patients. Synbiotics are generally safe and can be used in patients with advanced stage CKD. Synbiotic therapy improved gut dysbiosis, resulted improves tight junction expression and functions, and gut barrier<sup>21</sup>, leading to limitation of uremic toxin production and paracellular transport of toxins and phosphate. Our previous study reported that probiotic supplementation in rats with CKD had a decreased serum trimethylamine N-oxide (TMAO), a product of TMA that mediates atherosclerogenesis<sup>13</sup>. In the present study, our aim was to elucidate the benefit of synbiotic treatment in the lowering of serum phosphate and parathyroid hormones. *Lactobacillus casei* was used as the standard probiotic (STDPro) because it is a widely recognized probiotic strain commonly found in commercial probiotic products.

In our study, rats with cisplatin-induced CKD had high serum levels of creatinine, indoxyl sulfate and lower expression of jejunal ZO-1, suggesting the leaky gut syndrome. In terms of phosphate metabolism, hyperphosphatemia, high calcium-phosphorus product, which indicated the risk of VC, and hyperparathyroidism. Although calcification in the arterial walls was not detected in these rats, we believe that it was due to the insufficient duration of disease in this experiment. Treatment with STDPro slightly mitigated hyperphosphatemia in week 4 and week 8, but at the end of the experiment, STDPro could not improve any abnormal indicators found in CKD rats.

The synbiotics used in the present study were designed mainly to promote tight junction expression and functions. CKD rats treated with synbiotics had a high serum creatinine similar to CKD rats, but the expression of ZO-1 was markedly increased. Additionally, a decrease in serum phosphate, calcium phosphorus product and serum parathyroid levels was observed in Synbiotic rats, suggesting a reduced risk of MBD and VC in CKD rats. We hypothesized that the phosphate lowering effect of the synbiotics is due to the enhancement of tight junction protein expression and function, which limits the paracellular transport of phosphate (Fig. 5). According to our research, this is the first study to show the benefits of probiotic/synbiotic therapy in the serum phosphate control in CKD model.

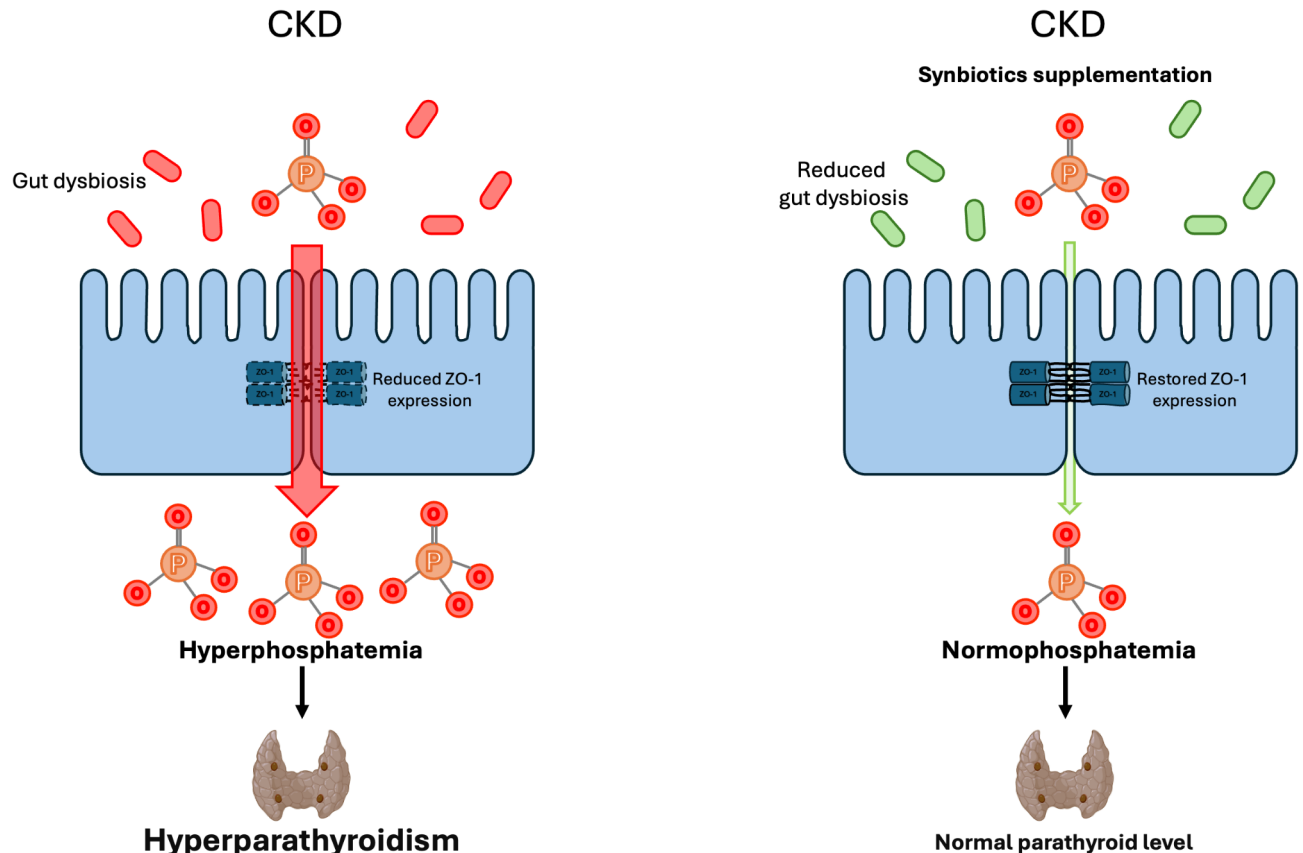


**Fig. 5.** Schematic overview the mechanism of synbiotic treatment in alleviation of hyperphosphatemia and hyperparathyroidism.

Another benefit of synbiotics is to modulate gut dysbiosis, as we found a significant difference in gut microbial profiles between CKD versus synbiotic rats. However, previous studies revealed that the patterns of gut dysbiosis in CKD were varied and inconsistent. For example, Cao C. (2022) reviewed that high abundances of Verrucomicrobia, Fusobacteria, Proteobacteria and *Escherichia Shigella*, while low abundances of Actinobacteria, Prevotella, Firmicutes, and *Faecalibacterium prausnitzii* are common in CKD patients, but Lactobacilli, *Clostridium*sensu stricto, Roseburia, Lachnospiraceae and other bacterial genera are varied<sup>25</sup>. According to this, intestinal microbial alteration in our study, including the decreased abundance of 11 genera and increased abundance of 18 genera, could not be assumed to be exclusively beneficial. For example, several bacteria, particularly *Escherichia coli*, *Clostridium* sp., and *Bacteroides* sp. contain tryptophanase, an important enzyme to convert tryptophan into indole, which is the precursor of indoxyl sulfate<sup>26</sup>. In our study, synbiotic treatment caused a lower abundance of *Clostridium* but a higher abundance of *Bacteroides*, and the production of indole and indoxyl sulfate was unpredictable. However, synbiotic rats had significantly lower serum indoxyl sulfate compared to untreated rats, showing that the modulation of gut dysbiosis by synbiotics is beneficial for reducing serum uremic toxin, either due to directly inhibit the toxin production, or indirectly limits intestinal barrier leakage.

The limitations of the present study are (1) we were unable to demonstrate the beneficial effects of synbiotics in the prevention of MBD and VC. To elucidate this, we require either induce higher degree of kidney injury or extend the duration of experiment. (2) The combination of two probiotic strains raises the arguable question of its necessity. We considered that one of these probiotic strains is capable of promoting the tight junction, but the combination of two strains is believed to have synergistic effect in improving intestinal microbiota modulation and providing a beneficial boarder spectrum<sup>27</sup>. (3) We could not directly measure the paracellular transport of phosphate in living rats. The assumption of the decreased paracellular transport based on the increase of intestinal tight junction demonstrated in this study. (4) The long term effect in lowering phosphate derived from synbiotic treatment, especially after the cessation of the supplementation, is crucial. We have planned to test this synbiotic in patients with CKD to determine its efficacy and safety.

## Conclusion

Supplementation of the synbiotics, comprised of *L.salivarius* LBR228, *B. longum* BFS309, FOS, and COS, effectively reduced serum phosphate, the calcium-phosphorus product, and PTH levels in rats with CKD, indicating the reduction of the risk of mineral bone disease and vascular calcification. These advantages are contributed by modulation of the gut microbiota and the improvement of tight junction protein expression. This



is the first study to show the benefit of synbiotic supplementation in serum phosphate and parathyroid control in an animal with CKD model.

## Data availability

Data is provided within the manuscript or supplementary information files.

Received: 14 December 2024; Accepted: 18 February 2025

Published online: 03 March 2025

## References

- Isakova, T. et al. KDOQI US commentary on the 2017 KDIGO clinical practice guideline update for the diagnosis, evaluation, prevention, and treatment of chronic kidney Disease-Mineral and bone disorder (CKD-MBD). *Am. J. Kidney Dis.* **70**, 737–751. <https://doi.org/10.1053/j.ajkd.2017.07.019> (2017).
- Burton, J. O., Goldsmith, D. J., Ruddock, N., Shroff, R. & Wan, M. Renal association commentary on the KDIGO (2017) clinical practice guideline update for the diagnosis, evaluation, prevention, and treatment of CKD-MBD. *BMC Nephrol.* **19**, 240. <https://doi.org/10.1186/s12882-018-1037-8> (2018).
- Cernaro, V., Longhitano, E., Casuscelli, C., Peritore, L. & Santoro, D. Hyperphosphatemia in chronic kidney disease: the search for new treatment paradigms and the role of Tenapanor. *Int. J. Nephrol. Renovasc Dis.* **17**, 151–161. <https://doi.org/10.2147/IJNRD.S385826> (2024).
- Ding, X. et al. Ferric citrate for the treatment of hyperphosphatemia and iron deficiency anaemia in patients with NDD-CKD: a systematic review and meta-analysis. *Front. Pharmacol.* **15**, 1285012. <https://doi.org/10.3389/fphar.2024.1285012> (2024).
- Via, R., Cortes, D. D. P., Druke, T. B. & Moyses, R. M. A. Persistent uncertainties in optimal treatment approaches of secondary hyperparathyroidism and hyperphosphatemia in patients with chronic kidney disease. *Curr. Osteoporos. Rep.* **22**, 441–457. <https://doi.org/10.1007/s11914-024-00881-3> (2024).
- Knopfel, T. et al. Paracellular transport of phosphate along the intestine. *Am. J. Physiol. Gastrointest. Liver Physiol.* **317**, G233–G241. <https://doi.org/10.1152/ajpgi.00032.2019> (2019).
- Wagner, C. A. The basics of phosphate metabolism. *Nephrol. Dial Transpl.* **39**, 190–201. <https://doi.org/10.1093/ndt/gfad188> (2024).
- King, A. J. et al. Inhibition of sodium/hydrogen exchanger 3 in the Gastrointestinal tract by Tenapanor reduces paracellular phosphate permeability. *Sci. Transl. Med.* **10** <https://doi.org/10.1126/scitranslmed.aam6474> (2018).
- Yang, X. et al. Characterization of gut microbiota in patients with stage 3–4 chronic kidney disease: a retrospective cohort study. *Int. Urol. Nephrol.* **56**, 1751–1762. <https://doi.org/10.1007/s11255-023-03893-7> (2024).
- Evenepoel, P., Stenvinkel, P., Shanahan, C. & Pacifici, R. Inflammation and gut dysbiosis as drivers of CKD-MBD. *Nat. Rev. Nephrol.* **19**, 646–657. <https://doi.org/10.1038/s41581-023-00736-7> (2023).
- Lambert, K. et al. Targeting the gut microbiota in kidney disease: the future in renal nutrition and metabolism. *J. Ren. Nutr.* **33**, S30–S39. <https://doi.org/10.1053/j.jrn.2022.12.004> (2023).
- Cabala, S., Ozgo, M. & Herosimczyk, A. The kidney-Gut Axis as a novel target for nutritional intervention to counteract chronic kidney disease progression. *Metabolites* **14** <https://doi.org/10.3390/metabo14010078> (2024).
- Anekal, W. et al. The usefulness of resistant maltodextrin and Chitosan oligosaccharide in management of gut leakage and microbiota in chronic kidney disease. *Nutrients* **15** <https://doi.org/10.3390/nu15153363> (2023).
- Hunthai, S. et al. Publisher correction: unraveling the role of gut microbiota by fecal microbiota transplantation in rat model of kidney stone disease. *Sci. Rep.* **14**, 29360. <https://doi.org/10.1038/s41598-024-78864-8> (2024).
- Tiranathanagul, K. et al. Comparative efficacy between Hemodialysis using super high-flux dialyzer with hemoperfusion and high-volume postdilution online hemodiafiltration in removing protein bound and middle molecule uremic toxins: A cross-over randomized controlled trial. *Artif. Organs.* **46**, 775–785. <https://doi.org/10.1111/aor.14161> (2022).
- Eslamifar, Z. et al. Ameliorative Effects of Gallic Acid on Cisplatin-Induced Nephrotoxicity in Rat Variations of Biochemistry, Histopathology, and Gene Expression. *Biomed Res Int* 2195238 (2021). <https://doi.org/10.1155/2021/2195238>
- Oberhuber, G., Granditsch, G. & Vogelsang, H. The histopathology of coeliac disease: time for a standardized report scheme for pathologists. *Eur. J. Gastroenterol. Hepatol.* **11**, 1185–1194. <https://doi.org/10.1097/00042737-199910000-00019> (1999).
- Thongpan, I. et al. Respiratory syncytial virus, human metapneumovirus, and influenza virus infection in Bangkok, 2016–2017. *PeerJ* **7**, e6748. <https://doi.org/10.7717/peerj.6748> (2019).
- Wang, Y. et al. Lactobacillus rhamnosus GG treatment potentiates intestinal hypoxia-inducible factor, promotes intestinal integrity and ameliorates alcohol-induced liver injury. *Am. J. Pathol.* **179**, 2866–2875. <https://doi.org/10.1016/j.ajpath.2011.08.039> (2011).
- Guo, X. et al. Polyamines are necessary for synthesis and stability of occludin protein in intestinal epithelial cells. *Am. J. Physiol. Gastrointest. Liver Physiol.* **288**, G1159–1169. <https://doi.org/10.1152/ajpgi.00407.2004> (2005).
- Chen, K. et al. Targeting gut microbiota as a therapeutic target in T2DM: A review of multi-target interactions of probiotics, prebiotics, postbiotics, and synbiotics with the intestinal barrier. *Pharmacol. Res.* **210**, 107483. <https://doi.org/10.1016/j.phrs.2024.107483> (2024).
- Hollander, D. & Kaunitz, J. D. The leaky Gut: tight junctions but loose associations?? *Dig. Dis. Sci.* **65**, 1277–1287. <https://doi.org/10.1007/s10620-019-05777-2> (2020).
- Iseri, K. et al. Bone mineral density and mortality in end-stage renal disease patients. *Clin. Kidney J.* **13**, 307–321. <https://doi.org/10.1093/ckj/sfaa089> (2020).
- Kidney Disease: Improving Global & Outcomes, C. K. D. M. B. D. U. W. G. KDIGO 2017 Clinical Practice Guideline Update for the Diagnosis, Evaluation, Prevention, and Treatment of Chronic Kidney Disease-Mineral and Bone Disorder (CKD-MBD). *Kidney Int Suppl* (**7**, 1–59 (2017). (2011). <https://doi.org/10.1016/j.kisu.2017.04.001>
- Cao, C., Zhu, H., Yao, Y. & Zeng, R. Gut dysbiosis and kidney diseases. *Front. Med. (Lausanne)*. **9**, 829349. <https://doi.org/10.3389/fmed.2022.829349> (2022).
- Gao, K., Mu, C. L., Farzi, A. & Zhu, W. Y. Tryptophan metabolism: A link between the gut microbiota and brain. *Adv. Nutr.* **11**, 709–723. <https://doi.org/10.1093/advances/nmz127> (2020).
- Kwoji, I. D., Aiyegoro, O. A., Okpeku, M. & Adeleke, M. A. Multi-Strain probiotics: synergy among isolates enhances biological activities. *Biology (Basel)*. **10**. <https://doi.org/10.3390/biology10040322> (2021).

## Acknowledgements

The authors express our sincere gratitude to Professor Dr. Intawat Nookeaw from Department Biomedical Informatics, University of Arkansas for Medical Sciences, Little Rock, Arkansas, USA, for his valuable guidance and meticulous proofreading of the manuscript, Assoc. Prof. Dr. Asada Leelahavanichkul from the Department of Microbiology, Faculty of Medicine, for his invaluable guidance in improving the techniques used in the animal experiments and Dr. Pajaree Chariyavilaskul from the Department of Pharmacology, Faculty of Medicine for

her invaluable assistance in conducting the laboratory tests for uremic toxins. Special thanks to Dr. Peerapat Visitchanakun for his assistance in handling the animals during the experiments. The authors also extend their appreciation to Mr. Tawatchai Chumponsuk, Miss Panadda, and Miss Tanyaporn Keratibumrungpong, scientists in the laboratory, for their support and facilitation throughout the research process. It is with deep sorrow that we acknowledge the passing of Mr. Panuwat Tansatian, a cherished friend and valued colleague. While his direct contributions to this research may have been limited, his unwavering support, insightful advice, and friendship played an invaluable role throughout our academic journey. His sudden and untimely departure has left an immense void in our hearts and in the lives of those who had the privilege of knowing him. We deeply mourn their loss and honor his memory with gratitude and profound respect.

### Author contributions

Conceptualization, W.A. and T.D.; Methodology, M.T., P.T. and M.K.; Software, W.A., N.C. and T.T.; Validation, N.C. and T.D.; Formal Analysis, T.D. and N.C.; Investigation, S.T. and M.T.; Resources, R.P., S.T. and T.D.; Data Curation, M.K., W.A. and N.C.; Writing—Original Draft Preparation, T.T. and W.A.; Writing—Review & Editing, T.D.; Visualization, W.A.; Supervision, N.C., and T.D.; Project Administration, T.D.; Funding Acquisition, T.D. All authors have read and agreed to the published version of the manuscript.

### Funding

The present study was financially supported by Rachadapiseksompode Fund, Chulalongkorn University (RA-MF-33/64 and GA65/33), the Fundamental Fund, Chulalongkorn University (HEA663000050), the Thailand Research Fund (TRF) (RSA280077), the Program Management Unit for Human Resources and Institutional Development, Research, and Innovation (PMU-B), grant number (B36G660010) and the Second Century Fund (C2F), Chulalongkorn University.

### Declarations

### Competing interests

The authors declare no competing interests.

### Additional information

**Supplementary Information** The online version contains supplementary material available at <https://doi.org/10.1038/s41598-025-91033-9>.

**Correspondence** and requests for materials should be addressed to T.D.

**Reprints and permissions information** is available at [www.nature.com/reprints](http://www.nature.com/reprints).

**Publisher's note** Springer Nature remains neutral with regard to jurisdictional claims in published maps and institutional affiliations.

**Open Access** This article is licensed under a Creative Commons Attribution-NonCommercial-NoDerivatives 4.0 International License, which permits any non-commercial use, sharing, distribution and reproduction in any medium or format, as long as you give appropriate credit to the original author(s) and the source, provide a link to the Creative Commons licence, and indicate if you modified the licensed material. You do not have permission under this licence to share adapted material derived from this article or parts of it. The images or other third party material in this article are included in the article's Creative Commons licence, unless indicated otherwise in a credit line to the material. If material is not included in the article's Creative Commons licence and your intended use is not permitted by statutory regulation or exceeds the permitted use, you will need to obtain permission directly from the copyright holder. To view a copy of this licence, visit <http://creativecommons.org/licenses/by-nc-nd/4.0/>.

© The Author(s) 2025